nature nanotechnology

ARTICLES

PUBLISHED ONLINE: 25 SEPTEMBER 2017 | DOI: 10.1038/NNANO.2017.168

Focal molography is a new method for the *in situ* analysis of molecular interactions in biological samples

Volker Gatterdam[1†], Andreas Frutiger[1†], Klaus-Peter Stengele[2], Dieter Heindl[2], Thomas Lübbers[3], Janos Vörös[1*] and Christof Fattinger[3*]

Focal molography is a next-generation biosensor that visualizes specific biomolecular interactions in real time. It transduces affinity modulation on the sensor surface into refractive index modulation caused by target molecules that are bound to a precisely assembled nanopattern of molecular recognition sites, termed the 'mologram'. The mologram is designed so that laser light is scattered at specifically bound molecules, generating a strong signal in the focus of the mologram via constructive interference, while scattering at nonspecifically bound molecules does not contribute to the effect. We present the realization of mologrames on a chip by submicrometre near-field reactive immersion lithography on a light-sensitive monolithic graft copolymer layer. We demonstrate the selective and sensitive detection of biomolecules, which bind to the recognition sites of the mologram in various complex biological samples. This allows the label-free analysis of non-covalent interactions in complex biological samples, without a need for extensive sample preparation, and enables novel time- and cost-saving ways of performing and developing immunoassays for diagnostic tests.

There are two major determinants that have to be fulfilled for the selective and sensitive detection of biomarkers in complex biological samples through specific binding (SB) to recognition sites: (1) high specificity and stability (slow off rate) of the recognition between the investigated biomolecules and (2) distinction of the specific recognition from nonspecific binding (NSB). In heterogeneous assays (for example, the classical enzyme-linked immunosorbent assay, or ELISA[1]), the specific molecular recognition occurs in close proximity to the solid phase, which is used for immobilization of the recognition element. The solid phase of a heterogeneous assay serves two fundamental functions: (1) display of the immobilized recognition site to the sample of interest and (2) retaining exposure of the recognition site to the washing solution during the washing step. Heterogeneous immunoassays in complex biological samples rely on intensive washing of the assay surface, which permits the specific binding signal obtained from the recognition event to be distinguished from signals that arise from NSB of the assay and sample components. Nanometre-sized defects in surface order and molecule orientation may expose unwanted chemical groups at the surface–solution interface, resulting in undesirable or uncontrollable surface properties enhancing NSB[2]. New methods to separate these NSB events from the molecular recognition are pivotal for selective and sensitive detection of biomolecules.

In visible light, molecules in aqueous solutions can manifest themselves either through modulation of the amplitude of the incident light (absorbing molecules, such as a dye), through modulation of the phase of the incident light by their refractive index, or by emitting fluorescent light[3]. With a few exceptions, biomolecules in water represent pure phase objects (no absorption) and manifest themselves only by their refractive index[4]. Therefore, many optical biosensors have been developed to measure the amount of proteins based on refractive index change, which means that all of them also detect non-specifically bound molecules[5–7].

Current state-of-the-art assay methods[8] typically deal with the NSB problem by using sandwich assays that allow the discrimination of the specifically bound secondary binders from the NSB molecules by extensive rinsing (using the difference in off rate) or by shear force (which discriminates the different binding strengths) in so-called force-discrimination assays[9,10]. Other label-free techniques like surface plasmon resonance (SPR)[11] or Mach–Zehnder[12] interferometry rely heavily on reference channels to obtain meaningful results. Owing to the spatial separation of the two channels, these methods require sophisticated set-ups and are also more prone to variations and gradients. The cantilever-based nanomechanical detection method of Zhang *et al.*[13] also requires reference probes and only enables sensitive measurements under static conditions. The method is not compatible with flow, or detection in a complex environment like an *in situ* cell culture measurement. On the other hand, the detection method described by Stern *et al.*[14] requires a purification step before detection of the analyte. It therefore does not allow direct study of the biomolecular interactions in the native complex sample environment.

There are very few existing concepts that can directly discriminate between SB and NSB (for example, the biomimetic approach presented by Cornell *et al.*[15] using ion channels, the molecular diffraction gratings introduced by Tsay *et al.*[16] and Cleverley *et al.*[17], or the recently introduced single-molecule techniques such as kinetic fingerprinting[18] that discriminate SB from NSB based on residence time and corresponding statistical parameters[19]). However, none of these are available in the current diagnostic market, possibly owing to the complexity of the required surface architecture or instrumentation.

Here, we present a realization of focal molography, a technique that can discriminate SB and NSB and is also sensitive and simple

[1]Laboratory of Biosensors and Bioelectronics, Institute for Biomedical Engineering, ETH Zurich, 8092 Zurich, Switzerland. [2]Roche Diagnostics GmbH, 82377 Penzberg, Germany. [3]Roche Pharma Research and Early Development, Roche Innovation Center Basel, 4070 Basel, Switzerland. †These authors contributed equally to this work. *e-mail: janos.voros@biomed.ee.ethz.ch; christof.fattinger@roche.com

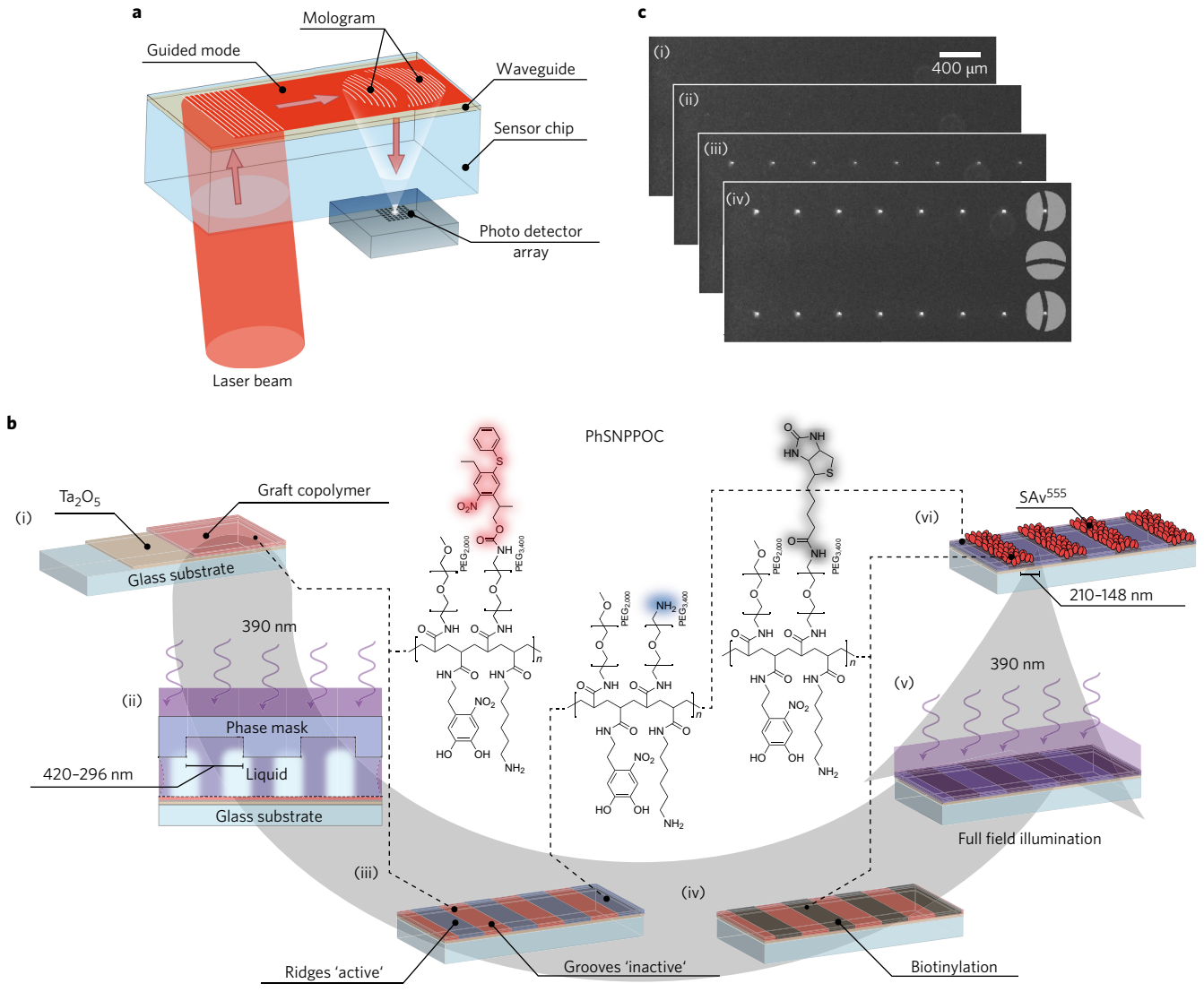

Figure 1 | Schematic illustration of the fundamental components of focal mology and the submicrometre near-field lithographic process used in mology. a, The sensor chip is based on a single-mode optical waveguide with a grating coupler. The guided mode is diffracted at the mologram and focused to a diffraction-limited spot. The central curved recess area in the mologram prevents the second-order Bragg reflection (for details see ref. 20). The spot intensity, which correlates quadratically with the bound mass of the analyte, is detected by a photodetector array. For details of the chip and readout configuration see Supplementary Figs 1 and 2. **b**, For a better understanding, the copolymer structures at different stages of the process are connected via dashed lines. (i) The 145 nm metal oxide (Ta_2O_5) layer is coated with a thin photosensitive graft copolymer layer containing PhSNPPOC protected amino-PEG_{3400} polymer. (ii) Phase mask technology is used for activation of the monolithic photosensitive layer. The physics of the phase mask lithography process results in structures with half the period of the phase mask (420–296 nm). This allows the creation of the nanostructures (210–148 nm line width) of the mologram: [NH_2|NH-PhSNPPOC] (see Supplementary Section 'Nomenclature of affinity modulation and surface composition of mologrammes'). (iii) Induced activation contrast after photolithography. Activated areas are termed 'ridges' and inactive areas 'grooves'. (iv) Further functionalization with amine reactive compounds leads to the desired binding properties (chemical functionalization). NHS-biotin for streptavidin (SAv) binding: [NH-biotin|NH-PhSNPPOC]. (v) To minimize the difference in NSB between grooves and ridges, or to realize backfilling of the mologram, the remaining PhSNPPOC groups are photocleaved. Additional passivation (not shown) can be obtained by amine reactive blocking reagents, for example, NHS-PEG. (vi) The mologramphic signal is generated by binding of SAv: [NH-biotin/SAv|NH_2]. **c**, Images showing the mologramphic raw data at four exemplary time points. The drawn mologrammes are an illustrated overlay and are invisible in reality. The middle row of the mologram overlay is 90° rotated and does not generate a signal. Because this pattern is incoherent with regard to the direction of the guided wave, the structure generates no diffractive signal, although, biochemically, the same molecular interaction takes place.

enough to potentially make it to the diagnostic market. The concept of focal mology was described recently[20]. Briefly, in focal mology, coherent laser light is diffracted at a coherent assembly of interaction sites (Fig. 1a). The coherent assembly comprises a precise submicrometre pattern of identical interaction sites that needs to be phase-matched to the incident coherent light over the entire pattern. The light diffracted at this assembly constructively interferes in a diffraction-limited focal spot (Airy disc). A molecular assembly with these properties is termed a 'mologram'. In essence, a mologram is a synthetic hologram composed of molecules, which scatters light into a diffraction-limited focal spot and is tuned such that it allows molecular interaction analysis. Acquisition of the mologramphic signal is realized through detection of the diffracted coherent light in the focus of

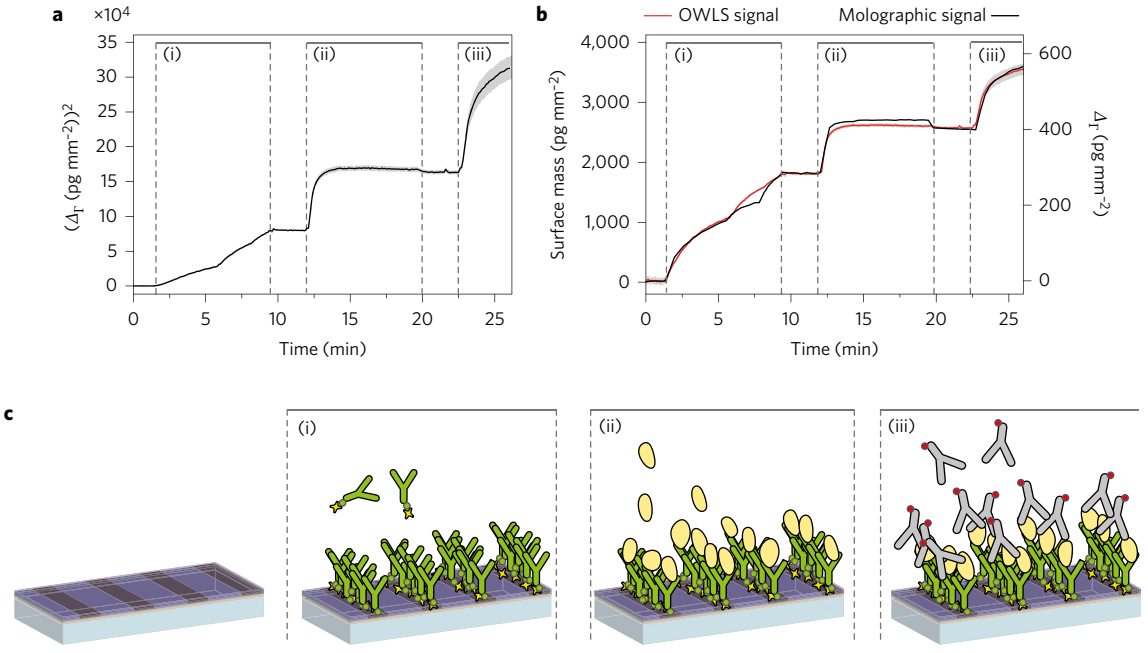

Figure 2 | Comparison of sandwich immunoassay performed by mology and OWLS (diffractometric versus refractometric biosensor). **a**, (i) Immobilization of SAv and biotinylated anti-TSH F(ab′)$_2$. (ii) Immobilization of the target hormone TSH. (iii) Signal enhancement by a second anti-TSH IgG. (For a full explanation of data processing, see Supplementary Figs 4 and 5). The signal consists of nine mologrames represented with the barely visible standard deviation (s.d.) as a grey ribbon. **b**, The linear signal overlaps with the OWLS signal at multiple key points. **c**, Schematic representation of the performed immuno-sandwich assay.

the mologram. The light intensity in the molographic focus scales quadratically with the surface mass density modulation Δ_Γ of the mologram. Background scattering by molecules that are randomly attached to the assay surface is intrinsically separated by focal mology from the coherent molographic signal. In addition, mology does not require the presence of a label, as in ELISA assays. Label-free mology visualizes biomolecular recognition events through the detection of minute phase-contrast changes in the nanoenvironment of the recognition sites in the mologram[20]. This opens up new perspectives and possibilities in analysing non-covalent interactions and especially in the discovery of unknown biomolecules in complex biological samples by pulldown assays[20].

In the challenging case of measuring biological responses and interactions directly in living tissue or cell cultures, most bioanalytical methods face severe problems with background signals or involve laborious referencing procedures. Although some methods (fluorescence-based techniques such as Förster resonance energy transfer (FRET) or the radiolabel-containing LigandTracer technology[21,22]) bypass some of these problems, they may disturb the studied molecular interactions as a result of staining or other interfering labels. In contrast, focal mology transforms the invisible affinity modulation of the mologram into refractive index modulation, inducing a focused beam of light[20,23], where the affinity modulation Δ_A is the difference in recognition site density for the target molecule between ridges and grooves. The sensitivity of most current biosensors is fundamentally limited by NSB events[24], but this novel analytical method enables the collective and sensitive discrimination of specific biomolecular recognition from NSB on a solid surface in heterogeneous assays. Focal mology achieves this by minimizing separation of the sensing and reference channel to its extreme—to less than the wavelength of light—while several hundreds of referencing and signal areas are embedded into a single sensing spot.

Here, we present the experimental realization of focal mology and the synthesis of mologrames on a biosensor chip by submicrometre near-field reactive immersion lithography (RIL) on a light-sensitive monolithic graft copolymer layer. For the first time, we demonstrate an emerging molographic signal that evolves in real time from a weak background (Fig. 1c and Supplementary Movie). We have developed a surface chemistry that enables the fabrication of mologrames on an optical waveguide by using a simple-to-use phase mask process, which allows submicrometre photopatterning of a non-fouling graft copolymer under immersion on a laboratory bench. This allows the tuning of surface chemistries specific to the desired analytical application. We also characterized the lithography process in detail with simulations and stimulated emission and depletion (STED) microscopy.

To demonstrate the capabilities of focal mology we will outline pivotal experiments with complex biological samples. We will first show that the technology has all the capabilities of refractometric sensors by performing a classical sandwich immunoassay. Second, we will describe a label-free assay (β-amyloid peptide) where we compare the binding behaviour in buffer and diluted serum. Third, we will demonstrate the unique properties and clinical relevance of focal mology by acquiring real-time label-free binding curves of a therapeutic antibody in human plasma samples. Finally, we have recorded the production of antibodies in a hybridoma cell culture *in situ* over long time periods. These are complex experiments that are hard to achieve using other label-free detection methods, which mainly can only measure large changes (that is, cell growth or morphology). In addition, state-of-the-art label-free detection methods often fail to successfully perform biomolecular interaction analysis in the presence of large amounts of background proteins or living cells. However, thanks to the inherent self-referencing of mology, we were able to obtain meaningful label-free data of molecular binding over long time periods in complex solutions, even without temperature stabilization[25]. For these reasons, we believe that focal mology has the potential to become the future label-free method of choice to study a large variety of biomolecular recognition and interaction processes in complex biological media on a sensor chip in real time—for example, the relation between protein secretion and cellular responses such as apoptosis[26,27].

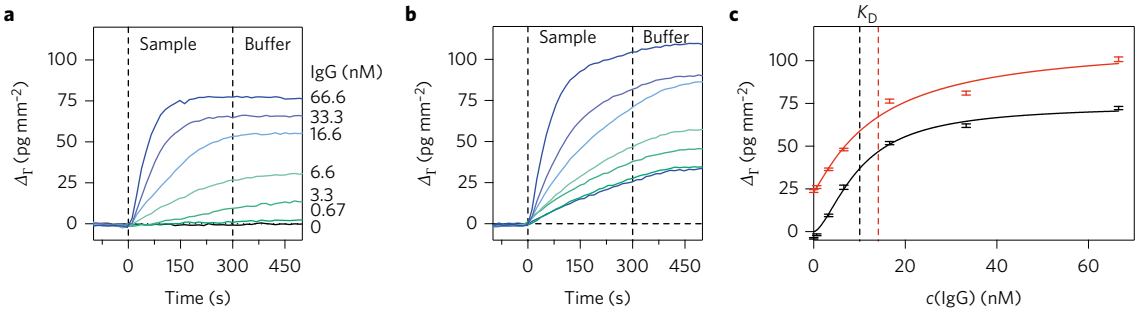

Figure 3 | Determination of assay specific affinity for antibody binding to β-amyloid peptide. a, Injection of an antibody against immobilized β-amyloid peptide, followed by washing with buffer. **b**, Repetition of the experiment with antibody in 20% horse serum. Both data sets show the raw unreferenced mographic signal. **c**, Determination of K_D in running buffer and serum. Endpoint values of the binding experiment in PBS-T buffer (t = 450 s) are represented by black bars and in serum by red bars in PBS-T buffer. Error bars represent the standard error of the mean (s.e.m.) of eight mograms. *c*, concentration.

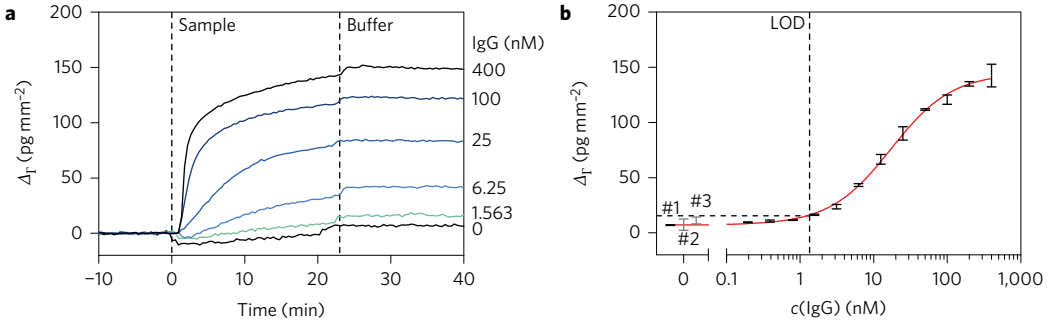

Figure 4 | Real-time detection of a therapeutic antibody in human plasma. a, Association and dissociation curves of a therapeutic antibody against an immobilized idiotypic antibody, displayed as mean signals of at least eight mograms normalized to the bound signal of the ideotypic antibody. The data are not baseline-corrected and therefore represent the raw data signal. **b**, Logarithmic representation of therapeutic antibody concentration against endpoint values for determination of LOD at three times the s.d. of the endpoint value of three different donor blanks.

To perform a meaningful mographic measurement, a few instrumentation requirements need to be satisfied. Focal mography requires a suitable dark-field illumination of the mogram, which was realized here by the guided mode of a high-refractive-index thin-film optical waveguide (Fig. 1a)[20,23]. This assures a high signal-to-background ratio. Mography also needs a submicrometre-scale coherent pattern of recognition sites, which can be created by a variety of existing biological lithography methods that were developed for biochips[28]. Here, this coherent pattern was fabricated by photolithography, as described for biotin[29,30], nanoparticles[31] or peptide synthesis[32]. For mography we used a new photoactivatable graft copolymer, similar to the graft copolymers recently described by Serrano *et al.*[33], to coat the tantalum pentoxide (Ta_2O_5) thin-film optical waveguide[34] (see Supplementary Information). The novel copolymer that we designed for mography has four key properties. (1) Before photolithographic exposure, the copolymer layer on the assay surface is monolithic and homogeneous, both in terms of its chemical and optical properties. The monolithic layer does not contain coherently arranged molecules, so it shows no mographic signal before the photolithography step. (2) The copolymer layer is resistant to nonspecific protein adsorption. However, as with any other protein-repellent surface, this copolymer layer exhibits defects and irregularities on the nanometre scale, which cause residual NSB to the assay surface[2,35]. Because these defects are not coherently arranged, they do not contribute to the mographic signal. (3) The copolymer layer contains a photoactivatable functional group for formation of the recognition sites by exposure to light. It is important to note that photolithography at a wavelength of 390 nm, at the energy doses used, does not induce coherent defects in the copolymer layer. (If it did, we would measure a signal from NSB to photo-induced defects in the whole-blood experiment presented in Supplementary Fig. 10a.) (4) The formed copolymer adlayer allows necessary chemical and biochemical modifications after initial surface coating.

The mographic pattern on the assay surface was created by submicrometre near-field RIL at 390 nm wavelength[36] (Fig. 1b and Supplementary Fig. 1). This wavelength is compatible with biological systems; for example, it does not induce structural changes in biomolecules. The submicrometre resolution of the photolithography step was realized by means of phase-mask technology[37,38]. Illumination through the phase mask results in activated curved lines called 'ridges', and inactive lines, in between, termed 'grooves'. Using this method, a coherent mographic assembly of recognition sites can be generated on the assay surface. For a more detailed characterization of the mogram and an explanation of the mogram's nomenclature, see Supplementary Section 'Nomenclature of affinity modulation and surface composition of mograms'.

Sandwich immunoassay

As a proof of principle that the technology has all the capabilities of state-of-the-art label-free refractometric sensors, we detected thyroid stimulating hormone (TSH) in a label-free, as well as a sandwich-type, manner. For comparison purposes, the experiment was conducted in parallel on a refractometric optical waveguide lightmode spectroscopy (OWLS) sensor system[39]. To allow for real-time observation and determination of the binding kinetics, a fluidic cell was designed for the following experiments (Supplementary Fig. 3b). Figure 2 shows the performed immunoassay based on mographic (Fig. 2a) and OWLS detection (Fig. 2b) as well as a schematic of the assay steps (Fig. 2c). A SAv/biotinylated $F(ab)_2$ precomplex was first bound to a

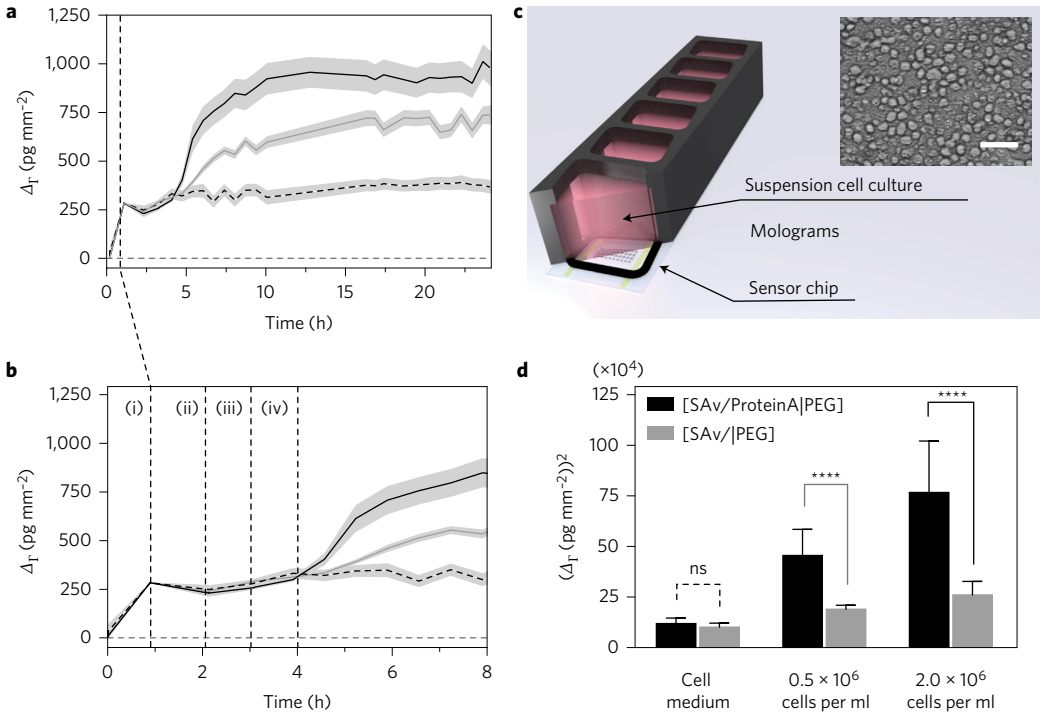

Figure 5 | *In situ* measurement of secreted immunoglobulins in a hybridoma cell culture. Four identical molographic chips were functionalized with biotinylated Protein A and non-functionalized (SAv) in separate wells. **a**, Real-time mass density increase during *in situ* measurement. Comparing the signal increase between the chip with (black curve, 2.0×10^6 cells ml^{-1}; grey curve, 0.5×10^6 cells ml^{-1}) and without (dashed curve) cells shows the production of proteins that bind to Protein A. The random signal spikes are artefacts due to imprecise repositioning of the instrument and hence different in-coupling efficiencies of the grating coupler while serial scanning of the different flow channels and chips. **b**, Zoom-in to the first part of the real-time binding curve, which was used for SAv normalization of the different chips (i). In half of the flow chambers, SAv was removed by DMSO injection and substituted with SAv/Protein A (ii). At time point (iii) the cell culture medium was added and at (iv) the cells were added. **c**, A bright-field microscopy image demonstrating the compatibility of mography with a high cell density on the sensor surface. Scale bar, 40 μm. **d**, Mass density increase by endpoint value measurement. Comparison of multiple endpoint values of a Protein A and a non-functionalized SAv molographic surface. The statistical difference for the cell-containing chips was significant. ****$P < 0.0001$; NS, not significant.

[NH-biotin|NH-PEG$_{12}$] mologram, followed by immobilization of the target hormone TSH and the secondary detection antibody. On taking the square root of the molographic signal, the two curves virtually overlap (Fig. 2b), illustrating the expected quadratic dependency of the molographic signal with the surface mass density modulation and hence the amount of bound molecules[20]. For practical reasons, we refer to Δ_Γ as the mass density modulation of the mologram. For an ideal canonic mologram[20], the value of Δ_Γ would be equal in size to the surface mass determined by OWLS. In reality, the modulation is smaller and therefore also the correlating Δ_Γ value. The OWLS signal after SAv binding (not shown) was used for normalization of the STED fluorescence signal, and the surface mass density modulation (283 pg mm^{-2} from STED) was used to normalize the molographic signal. A signal stability test and a negative control of the TSH assay (lacking the primary capture antibody) are presented in Supplementary Fig. 11. The key feature of robustness against incoherent influences such as temperature, buffer composition (Supplementary Fig. 11) and NSB makes mography promising for diagnostic applications.

Determining specific affinity in a direct binding assay in serum

Analysis of biomolecular interactions is one of the most important areas in life science. This is why label-free biosensors such as SPR are widely used in biochemistry and biology laboratories. However, routinely, these methods only work with purified samples. Samples that are more complex, like blood plasma, require a high amount of optimization and working time. Focal mography can offer a better option to obtain unique data on molecular interactions in biologically relevant solutions. As an example, we present a kinetic analysis between an antibody and the β-amyloid peptide, which is clinically relevant for the treatment of Alzheimer's disease with active or passive vaccination[40]. We demonstrate that the dissociation constant K_D of an antibody against β-amyloid can not only be determined in buffer, but also in serum. We injected different concentrations of the antibody in a flow cell containing a β-amyloid peptide modified assay surface (Fig. 3a). The expected concentration-dependent increase in the molographic signal intensity was observed. After 5 min, the association phase was interrupted, and buffer was introduced into the flow cell. The expected slow dissociation for the higher antibody concentrations was observed, while a small signal increase was found for lower concentrations. This can be explained by the non-optimized geometry of the used flow cell, because residual antibodies from corner areas were only slowly washed out of the system by the buffer. An identical experiment with the antibody spiked into 20% horse serum revealed a comparable binding behaviour (Fig. 3b). A K_D of 10.1 ± 0.5 nM in PBS-T and 14.1 ± 1.8 nM in serum could be derived from the equilibrium binding state (Fig. 3c). This first molographic example of real-time target binding and affinity determination in a complex biological fluid was performed without any referencing or additional surface-blocking steps. It therefore gives only a glimpse of what can be achieved in the future by focal mography.

Detection of a therapeutic antibody in human plasma

To show the usefulness of the technology in a potential clinical application we detected, in a label-free manner, the concentration

of a therapeutic antibody in a diluted human plasma sample. Assessing the therapeutic antibody concentration is key to determining the physiological half-life of a biopharmaceutical in the bloodstream of a patient. In our pioneering experiment, we fabricated a molographic chip containing an idiotypic capture antibody recognizing a therapeutic antibody. Human plasma samples spiked with different concentrations of this therapeutic antibody were used as a model system for potential patient samples. The compatibility of the molographic system with higher concentrations of the initial complex samples, in this case 10% plasma, enables a higher sensitivity towards the overall detection of low-abundant plasma proteins. Injection of diluted plasma samples exhibited the expected concentration-dependent increase in the molographic signal intensity (Fig. 4). Evaluation of the reproducibility of the measurements is summarized in Supplementary Table 3. It is noteworthy that the presented data for the β-amyloid and the therapeutic antibody are not reference-corrected, unlike the common practice for established biosensing systems[41]. Because, for refractometric biosensors, the signals caused by NSB are substantially larger than the specific binding signal, subtraction of NSB from the detected signal usually completely obscures the specific binding signal for clinically relevant concentrations of the analyte. In addition, the variation of NSB from patient to patient does not allow sensors to be calibrated, rendering most of the established techniques non-applicable for diagnostic tests[42]. Therefore, the intrinsic self-referencing, in combination with the low NSB of the copolymer surface, gives focal molography a unique advantage for operation in complex samples. Thanks to this robustness, and the possibilities for multiplexing, miniaturization and wash-free operation, one could even envision performing such interaction analyses with individualized treatment for every patient. For the underlying assay, the limit of detection (LOD) was determined at the stable binding phase during washing of the formed immune complex (Fig. 4a). Evaluation of the maximal binding signal in correlation with the concentration resulted in a reproducible LOD of 200 ng ml^{-1} (1.3 nM) as the detectable antibody concentration in human plasma (Fig. 4b). This is already similar to the performance of the best published data with state-of-the-art label-free SPR instruments for antibodies and cancer markers, which mainly determine the LOD in buffer[25,43].

The LOD is a relevant parameter for every diagnostic assay, as it defines the lowest analyte concentration that can be distinguished from the absence of the substance within a confidence limit (usually 99% or three sigmas)[44,45]. For a distinct immunometric assay, the LOD is expressed in terms of sample concentration (that is, ng ml^{-1}), whereas an assay independent LOD that characterizes the capabilities of the sensor technology can be obtained as the surface mass density modulation between ridges and grooves on the mologram (that is, pg mm^{-2})[46,47]. A surface load of 1 pg mm^{-2} corresponds to ~1 RU (RU: response unit) on the Biocore system (the gold standard for label-free detection; see ref. 20 and references therein). Scientists dealing with a broad variety of label-free sensor devices often use 'refractive index units' (RIU) instead of RUs. A sensor resolution of 10^{-6} RIU means that a refractive index change of 10^{-6} in the liquid on the sensor surface can be measured reliably. A surface load of 1 pg mm^{-2} (1 RU) in the aqueous running buffer corresponds to a change in RIU of $\sim 2 \times 10^{-6}$ RIU (see page 3 of ref. 20). The assay independent LOD of the molographic system was determined as three times the standard deviation of the molographic baseline before analyte injection. The presented experiment with three individual chips achieved a sensitivity of ~5 pg mm^{-2}. This value was obtained through normalization with the STED data and therefore only provided an upper limit bound of the LOD. These LOD values were already reasonable (the detection limit of SPR is currently between 0.1 and 1 pg mm^{-2} and was at 10–20 pg mm^{-2} in the early 1990s when the label-free SPR method was introduced)[25,47]. In such complex samples in particular, we expect that the LOD of focal molography can be improved by at least two orders of magnitude by further optimizing the lithography process and by using an optimized set-up for the molographic readout.

In situ cell culture measurements

Although several (some commercial) tools exist for monitoring the behaviour of living cells in an ensemble, these typically only provide information about morphological changes, and lack molecular specificity[48]. However, the robustness of focal molography allowed long-lasting, *in situ* measurements of secreted antibodies (IgG) produced by a hybridoma cell culture. Protein A, a 42 kDa surface protein originally found in the cell wall of the bacterium *Staphylococcus aureus*, was used as the binding partner to measure the secreted antibody, because it contains four high-affinity binding sites capable of interacting with he Fc region from IgG. The cells were cultured on the molographic chip in an open version of the flow chamber containing 500 µl of the cell culture (Fig. 5c). The sensor chip consisted of two separate mologram sets: [NH-biotin/SAv/Bi-Protein A|NH-PEG$_{12}$] (antibody-capturing mologram with biotinylated Protein A (Bi-Protein A)) and [NH-biotin/SAv|NH-PEG$_{12}$] (negative control). The chip was placed inside the ZeptoReader and the molographic signal was measured on a regular basis over 24 h. The experiment was performed with different cell densities and in replicates of at least three. As expected, different molographic responses could be seen for the negative control and also for the different cell densities (Fig. 5a,b,d).

Conclusion

In summary, we have demonstrated the realization of focal molography as a new bioanalytical technique, which distinguishes itself from other techniques by its insensitivity to NSB, resulting in robustness and wide applicability. In all studies that investigate molecular recognition and binding, the molographic biosensor principle is of great interest because it allows for label-free detection of trace amounts of all kinds of biomolecules (for example, hormones, chemokines, cytokines and interleukins) in real biological samples (for example, serum, plasma or the supernatant of *in vitro* cell culture experiments). This new method thus opens up possibilities in many areas of biology, such as the monitoring of cell–cell communication, secretion of biomolecules and also cell surface interactions. Owing to its simplicity, robustness and potential for miniaturization, focal molography will also have an impact on the development of future hand-held point-of-care diagnostic devices.

Methods

Methods and any associated references are available in the online version of the paper.

Received 13 January 2017; accepted 11 July 2017;
published online 25 September 2017

References

1. Engvall, E. & Perlmann, P. Enzyme-linked immunosorbent assay (ELISA) quantitative assay of immunoglobulin G. *Immunochemistry* **8,** 871–874 (1971).
2. Love, J. C., Estroff, L. A., Kriebel, J. K., Nuzzo, R. G. & Whitesides, G. M. Self-assembled monolayers of thiolates on metals as a form of nanotechnology. *Chem. Rev.* **105,** 1103–1169 (2005).
3. Shimomura, O. The discovery of aequorin and green fluorescent protein. *J. Microsc.* **217,** 3–15 (2005).
4. McMeekin, T. L., Groves, M. L. & Hipp, N. J. in *Amino Acids and Serum Proteins* Vol. 44 (ed. Stekol, J. A.) 54–66 (American Chemical Society, 1964).
5. Vörös, J. The density and refractive index of adsorbing protein layers. *Biophys. J.* **87,** 553–561 (2004).
6. Homola, J. Present and future of surface plasmon resonance biosensors. *Anal. Bioanal. Chem.* **377,** 528–539 (2003).
7. Brolo, A. G. Plasmonics for future biosensors. *Nat. Photon.* **6,** 709–713 (2012).

8. Wilson, R. Sensitivity and specificity: twin goals of proteomics assays. Can they be combined? *Expert Rev. Proteomics* **10,** 135–149 (2013).
9. Lee, G. U., Metzger, S., Natesan, M., Yanavich, C. & Dufrene, Y. F. Implementation of force differentiation in the immunoassay. *Anal. Biochem.* **287,** 261–271 (2000).
10. Mulvaney, S. P. *et al.* Rapid, femtomolar bioassays in complex matrices combining microfluidics and magnetoelectronics. *Biosens. Bioelectron.* **23,** 191–200 (2007).
11. Myszyka, D. G. Improving biosensor analysis. *J. Mol. Recognit.* **12,** 279–284 (1999).
12. Kozma, P., Kehl, F., Ehrentreich-Förster, E., Stamm, C. & Bier, F. F. Integrated planar optical waveguide interferometer biosensors: a comparative review. *Biosens. Bioelectron.* **58,** 287–307 (2014).
13. Zhang, J. *et al.* Rapid and label-free nanomechanical detection of biomarker transcripts in human RNA. *Nat. Nanotech.* **1,** 214–220 (2006).
14. Stern, E. *et al.* Label-free biomarker detection from whole blood. *Nat. Nanotech.* **5,** 138–142 (2010).
15. Cornell, B. A. *et al.* A biosensor that uses ion-channel switches. *Nature* **387,** 580–583 (1997).
16. Tsay, Y. G. *et al.* Optical biosensor assay (OBA). *Clin. Chem.* **37,** 1502–1505 (1991).
17. Cleverley, S., Chen, I. & Houle, J. F. Label-free and amplified quantitation of proteins in complex mixtures using diffractive optics technology. *J. Chromatogr.* **878,** 264–270 (2010).
18. Johnson-Buck, A. *et al.* Kinetic fingerprinting to identify and count single nucleic acids. *Nat. Biotechnol.* **33,** 730–732 (2015).
19. Gunnarsson, A. *et al.* Drug discovery at the single molecule level: inhibition-in-solution assay of membrane-reconstituted β-secretase using single-molecule imaging. *Anal. Chem.* **87,** 4100–4103 (2015).
20. Fattinger, C. Focal mology: coherent microscopic detection of biomolecular interaction. *Phys. Rev. X* **4,** 031024 (2014).
21. Gedda, L., Björkelund, H. & Andersson, K. Real-time immunohistochemistry analysis of embedded tissue. *Appl. Radiat. Isot.* **68,** 2372–2376 (2010).
22. Bondza, S., Stenberg, J., Nestor, M., Andersson, K. & Bjorkelund, H. Conjugation effects on antibody–drug conjugates: evaluation of interaction kinetics in real time on living cells. *Mol. Pharm.* **11,** 4154–4163 (2014).
23. Binnig, G. Coherent signal picks out biomolecular interactions. *Physics* **7,** 84 (2014).
24. Woolley, C. F., Hayes, M. A., Mahanti, P., Douglass Gilman, S. & Taylor, T. Theoretical limitations of quantification for noncompetitive sandwich immunoassays. *Anal. Bioanal. Chem.* **407,** 8605–8615 (2015).
25. Homola, J. Surface plasmon resonance sensors for detection of chemical and biological species. *Chem. Rev.* **108,** 462–493 (2008).
26. Ashkenazi, A. & Dixit, V. M. Death receptors: signaling and modulation. *Science* **281,** 1305–1308 (1998).
27. Jemmerson, R., LaPlante, B. & Treeful, A. Release of intact, monomeric cytochrome *c* from apoptotic and necrotic cells. *Cell Death Differ.* **9,** 538–548 (2002).
28. Jonkheijm, P., Weinrich, D., Schröder, H., Niemeyer, C. M. & Waldmann, H. Chemical strategies for generating protein biochips. *Angew. Chem. Int. Ed.* **47,** 9618–9647 (2008).
29. Pirrung, M. C. & Huang, C. Y. A general method for the spatially defined immobilization of biomolecules on glass surfaces using 'caged' biotin. *Bioconjug. Chem.* **7,** 317–321 (1996).
30. Sundberg, S. A. *et al.* Spatially-addressable immobilization of macromolecules on solid supports. *J. Am. Chem. Soc.* **117,** 12050–12057 (1995).
31. Vossmeyer, T., DeIonno, E. & Heath, J. R. Light-directed assembly of nanoparticles. *Angew. Chem. Int. Ed.* **36,** 1080–1083 (1997).
32. Fodor, S. P. *et al.* Light-directed, spatially addressable parallel chemical synthesis. *Science* **251,** 767–773 (1991).
33. Serrano, Â., Zürcher, S., Tosatti, S. & Spencer, N. D. Imparting nonfouling properties to chemically distinct surfaces with a single adsorbing polymer: a multimodal binding approach. *Macromol. Rapid Commun.* **37,** 622–629 (2016).
34. Schmitt, K., Oehse, K., Sulz, G. & Hoffmann, C. Evanescent field sensors based on tantalum pentoxide waveguides—a review. *Sensors* **8,** 711–738 (2008).
35. Pasche, S., De Paul, S. M., Vörös, J., Spencer, N. D. & Textor, M. Poly(L-lysine)-graft-poly(ethylene glycol) assembled monolayers on niobium oxide surfaces: a quantitative study of the influence of polymer interfacial architecture on resistance to protein adsorption by ToF-SIMS and *in situ* OWLS. *Langmuir* **19,** 9216–9225 (2003).
36. Aizenberg, J., Rogers, J. A., Paul, K. E. & Whitesides, G. M. Imaging profiles of light intensity in the near field: applications to phase-shift photolithography. *Appl. Opt.* **37,** 2145–2152 (1998).
37. Tanaka, T. *et al.* A novel optical lithography technique using the phase-shifter fringe. *Jpn J. Appl. Phys.* **30,** 1131–1136 (1991).
38. Hill, K. O., Malo, B., Bilodeau, F., Johnson, D. C. & Albert, J. Bragg gratings fabricated in monomode photosensitive optical fiber by UV exposure through a phase mask. *Appl. Phys. Lett.* **62,** 1035 (1993).
39. Vörös, J. *et al.* Optical grating coupler biosensors. *Biomaterials* **23,** 3699–3710 (2002).
40. Panza, F. *et al.* Amyloid-based immunotherapy for Alzheimer's disease in the time of prevention trials: the way forward. *Expert Rev. Clin. Immunol.* **10,** 405–419 (2014).
41. Vaisocherová, H. *et al.* Ultralow fouling and functionalizable surface chemistry based on a zwitterionic polymer enabling sensitive and specific protein detection in undiluted blood plasma. *Anal. Chem.* **80,** 7894–7901 (2008).
42. Riedel, T. *et al.* Hepatitis B plasmonic biosensor for the analysis of clinical serum samples. *Biosens. Bioelectron.* **85,** 272–279 (2016).
43. Piliarik, M., Bocková, M. & Homola, J. Surface plasmon resonance biosensor for parallelized detection of protein biomarkers in diluted blood plasma. *Biosens. Bioelectron.* **26,** 1656–1661 (2010).
44. MacDougall, D. & Crummett, W. B. Guidelines for data acquisition and data quality evaluation in environmental chemistry. *Anal. Chem.* **52,** 2242–2249 (1980).
45. Armbruster, D. A. & Pry, T. Limit of blank, limit of detection and limit of quantitation. *Clin. Biochem. Rev.* **29**(Suppl. 1)**,** S49–S52 (2008).
46. Fan, X. *et al.* Sensitive optical biosensors for unlabeled targets: a review. *Anal. Chim. Acta* **620,** 8–26 (2008).
47. Kolomenskii, A. A., Gershon, P. D. & Schuessler, H. A. Sensitivity and detection limit of concentration and adsorption measurements by laser-induced surface-plasmon resonance. *Appl. Opt.* **36,** 6539–6547 (1997).
48. Horvath, R., Pedersen, H. C., Skivesen, N., Selmeczi, D. & Larsen, N. B. Monitoring of living cell attachment and spreading using reverse symmetry waveguide sensing. *Appl. Phys. Lett.* **86,** 071101 (2005).

Acknowledgements

The authors thank V. Guzenko (ETH) and W. Arens (IMT) for technical support in fabrication of the phase mask, S. Tosatti (SuSoS) and S. Zürcher (SuSoS) for consulting regarding surface science questions and production of the copolymer, A. Nichtl (Roche Diagnostics) for support with various reagents, H.P. Herzig (EPFL) and A. Naqavi (EPFL) for support with numerical simulations and J. Hehl and T. Schwarz (ScopeM/ETH) for STED support. For designing and fabricating numerous hardware components, the authors thank T. Kissling, R. Rietmann (Roche) and S. Wheeler (ETH). The authors also thank A. Lieb for support with ZeptoReader-related issues. The authors thank the following for discussions on various aspects of the project: M. Hennig, K. Mueller, M. Lauer, A. Rufer, G. Dernick, M. Marcinowski, M. Essenpreis, M. Hein, O. Gutmann, A. Drechsler, M. Glauser, N. Milicevic, J. Spinke, A. Maurer, C. Patsch, C. Cusulin, J. Fingerle, R. Staack and A. Poehler. The authors acknowledge the Roche Postdoc Fellowship (RPF) Program, ETH Zurich and the NCCR Molecular Systems Engineering for funding.

Author contributions

Experiments were designed by V.G., K.-P.S., D.H., T.L., J.V. and C.F. C.F. performed the calculations for the phase mask and all other optical components. Molographic experiments were performed by V.G. A.F. performed the numerical simulations and wrote the evaluation software with support from J.V. and C.F. All authors read and approved the manuscript for submission.

Additional information

Supplementary information is available in the online version of the paper. Reprints and permissions information is available online at www.nature.com/reprints. Publisher's note: Springer Nature remains neutral with regard to jurisdictional claims in published maps and institutional affiliations. Correspondence and requests for materials should be addressed to J.V. and C.F.

Competing financial interests

The authors declare no competing financial interests.

Methods

All chemicals were obtained from Sigma-Aldrich in at least analytical grade purity if not stated otherwise. PhSNPPOC chloroformate was purchased from Orgentis Chemicals. NHS-PEG_{12}-OMe was obtained from Iris Biotech. PBS buffer, streptavidin-AlexaFluor555 and streptavidin-AlexaFluor488 were obtained from Thermo Fisher Scientific, and the PBS buffer was dosed with 0.05% Tween20. The PAA-g-PEG-NH-PhSNPPOC copolymer used as a biocompatible coating was provided by SuSoS. Horse serum was provided by Roche Diagnostics. Human blood samples were obtained from Blutspende Zürich. All reactions were conducted in ultrapure MilliQ water (18.2 MΩ cm at 25 °C; Merck Millipore).

Establishing a suitable sensing layer for focal molography. The proper design of the molographic surface on the Ta_2O_5 thin-film optical waveguide was evaluated by optical waveguide lightmode spectroscopy (OWLS) with an OWLS 210 instrument from MicroVacuum (see Supplementary Section 'Focal molography compared to OWLS'). The refractometric OWLS technique is based on thin-film optical waveguide chips comparable with those used for focal molography. This allows direct transfer of the OWLS findings to chips designed for molography. OWLS chips were obtained from MicroVacuum and sputtered with 10 nm Ta_2O_5 at IMT. All cleaning and coating reactions were carried out in glassware or Teflon chambers. Chips were cleaned with toluene followed by isopropanol and MilliQ water, each step for 10 min in an ultrasonication bath. After blow drying and surface activation by a 2 min exposure to oxygen plasma (18 W, Harrick Plasma PDC-32G) the chip was immediately assembled in the flow chamber and flushed with running buffer. After baseline equilibration overnight, the desired OWLS experiment was conducted.

Preparation of sensor chips for focal molography. Thin-film optical waveguides with a 145 nm Ta_2O_5 layer were obtained from ZeptoSense. An optional prewash with 0.1% aqueous Tween20 solution assured removal of adsorbed proteins. Intensive washing with isopropanol and MilliQ water was used to remove organic environmental contaminations. Chips were then cleaned with highly oxidizing Piranha solution (H_2SO_4/H_2O_2 7:3) for 30 min. (Special precautions have to be taken for Piranha solution, which reacts explosively with organic material.) After excessive washing with MilliQ water, the chips were blow dried and activated by 2 min of oxygen plasma. After plasma treatment, the chips were immediately immersed in the PAA-g-PEG-NH-PhSNPPOC graft copolymer coating solution (0.1 mg ml^{-1} in 1 mM HEPES pH 7.3 for 20 min). After layer formation, the coated chips were cleaned with MilliQ water. To fully passivate the layer, dried chips were immersed in a 25 mM methyl chloroformate solution in anhydrous acetonitrile containing 2 equiv. *N*,*N*-diisopropylethylamine for 5 min. This step assured that all residual unbound primary amines from the polymeric backbone were not interfering with the photolithographic process of amine generation. The coated chips were washed with ethanol and MilliQ water, and blow dried by a nitrogen jet. Prepared sensor chips could be stored for several months in the dark at 4 °C until further use.

Photolithographic process for formation of molograms. Photolithography was conducted in a yellow-lit room (L58 W/62; Osram) to avoid unwanted photoactivation. To avoid 390 nm stray light during illumination, most parts of the illumination unit were fabricated with black non-reflecting surfaces. A copolymer-coated sensor chip was placed inside the illumination unit (Supplementary Fig. 1). After alignment of the chip and the phase mask (IMT) the micrometer-sized gap between chip and phase mask was filled with DMSO containing 0.1% aq. hydroxylamine. The photolithographic exposure at 390 nm was conducted with a BlueWave LED Prime UVA light source from DYMAX equipped with a light guide. Illumination was performed at a distance of 20 cm with the light source at full intensity (resulting in an averaged irradiation power of ~4.6 mW cm^{-2}). After gently separating the phase mask and chip and washing with ethanol and MilliQ water, the activated ridges were functionalized with amine reactive substances such as 1 mM sNHS-biotin. To minimize interference in the assay, any remaining PhSNPPOC groups were removed by full chip illumination (flood exposure) for 5 min under DMSO containing 0.1% hydroxylamine. An optional blocking step of photoactivated primary amines was either performed as described above with methyl chloroformate, or with a 1 mM aqueous NHS-PEG solution at pH 8.5.

Confocal laser scanning/STED microscopy. Confocal laser scanning microscopy images of AlexaFluor488-labelled streptavidin were recorded on a Zeiss LSM 510. STED microscopy images were taken on a Leica SP 8 STED microscope. Fluorescent streptavidin (AlexaFluor555) was excited at 555 nm with a white light laser and depleted at 660 nm by the STED laser. Images were deconvoluted with Huygens Professional and further processed with ImageJ/Fiji software and Python.

Molographic measurements. Thin-film optical waveguides carrying molograms were measured with the ZeptoReader[49] (ZeptoSense) at a wavelength of 635 nm for the incident and diffracted light, without any optical filter in the detection path. For more information on the ZeptoReader's mode of operation, see Supplementary Fig. 3. The object plane containing the molographic foci (900 μm below the molographic pattern on the chip) was imaged with the camera objective of the ZeptoReader. This distance marks the plane on which the three-dimensional voxels are located, where the diffracted light of all curved mologram lines positively interferes to a focal spot in space. Typical instrument parameters were as follows: image integration time of 1 s and a grey filter value of 0.001 in the illumination path of the ZeptoReader. For real-time evaluation of molographic data, automation (AutoHotkey) and evaluation (MATLAB) scripts were written.

Sandwich immunoassay (TSH). A precomplex of 100 nM SAv and 200 nM biotinylated anti-TSH F(ab′)2 in PBS-T buffer (0.05% Tween20) were incubated for 10 min before being immobilized at a [NH-biotin|NH-PEG_{12}] mologram. TSH was injected at a concentration of 20 μg ml^{-1} in PBS-T followed by formation of the sandwich complex by 20 μg ml^{-1} anti-TSH IgG. All reagents were provided by Roche Diagnostics.

Determining specific antibody affinity in a direct binding assay in serum. An antibody against the C terminus of the human β-amyloid (1–40) peptide was obtained from Abcam, and the corresponding biotinylated peptide was supplied by AnaSpec. A preformed complex of streptavidin and the N-terminal biotinylated β-amyloid (ratio 100:200 nM) was bound to a [NH-biotin|NH-PEG_{12}] mologram. Varying antibody concentrations ranging from 66.6 to 0.6 nM in PBS-T or 20% horse serum were injected with a flow of 50 μl min^{-1} in PBS-T running buffer (0.05% Tween 20), followed by regeneration by 10 mM glycine pH 2.0.

Therapeutic antibody detection in human plasma. Precomplex formation of 100 nM SAv and 30 nM biotinylated idiotypic capture antibody provided by Roche Diagnostics was performed in PBS-T buffer (0.05% Tween20) for at least 10 min. Immobilization of the complex was achieved on a [NH-biotin|NH-PEG12] mologram. Running buffer (PBS-T) was supplemented with 300 mM NaCl. Human plasma prepared from EDTA stabilized blood samples was spiked with a therapeutic antibody provided by Roche Diagnostics. A concentration series of the plasma sample ranging from 400 to 0.195 nM of the therapeutic antibody was prepared, followed by a 1:10 dilution with running buffer before analysis by focal molography in triplicate. Injections of the individual samples were carried out at 10 μl min^{-1} for 20 min. Concentrations were applied in the order high to low for the first series and randomly for the second and third replicates. A stabilized endpoint signal for LOD evaluation was achieved by washing at 50 μl min^{-1}. Between each analyte injection, the whole SAv precomplex was renewed by stripping the chip with pure DMSO followed by 8 M guanidine hydrochloride. To evaluate signal variations for various samples, lithography and plasma donor effects binding curves were evaluated in triplicate for each of the three parameters (see Supplementary Table 3).

***In situ* cell culture measurements.** A hybridoma cell culture line secreting glutathione S-transferase (GST) directed antibodies was provided by Roche Innovation Center Basel. The progression of antibody production was detected *in situ* by focal molography through binding to Protein A, which contains four high-affinity binding sites capable of interacting with the Fc region of IgG. For this purpose, we used an open well plate holder carrying four molographic sensor chips as a bottom plate. One well contained a [NH-biotin/SAv/Bi-Protein A|NH-PEG_{12}] mologram, and a second contained a control surface with a [NH-biotin/SAv|NH-PEG_{12}] pattern. Each of these three positive/negative pairs per chip was covered with only cell culture medium, 0.5×10^6 cells ml^{-1} or 2.0×10^6 cells ml^{-1}. Biotinylated Protein A was obtained from Thermo Fisher Scientific. Both wells were covered with cell culture medium, with or without cells, respectively. The cell-chip assembly with 6×4 experiments was monitored inside the ZeptoReader without further temperature or CO_2 control. Statistical analysis was conducted using two-way ANOVA. A P value of <0.05 was considered significant. For the statistical evaluation, at least 67 molograms were used.

Data availability. The data that support the findings of this study are available from the corresponding author upon reasonable request.

References

49. Pawlak, M. *et al.* Zeptosens' protein microarrays: a novel high performance microarray platform for low abundance protein analysis. *Proteomics* **2,** 383–393 (2002).